Express Polymer Letters Vol.17, No.2 (2023) 181–195
Available online at www.expresspolymlett.com
https://doi.org/10.3144/expresspolymlett.2023.13

Research article

Influence of different vulcanizing agents on structures and properties of sepiolite-filled natural rubber composites

Nabil Hayeemasae[1,2], *Siriwat Soontaranon*[3], *Abdulhakim Masa*[2,4*]

[1]Department of Rubber Technology and Polymer Science, Faculty of Science and Technology, Prince of Songkla University, Pattani Campus, 94000 Pattani, Thailand
[2]Research Unit of Advanced Elastomeric Materials and Innovations for BCG Economy (AEMI), Faculty of Science and Technology, Prince of Songkla University, Pattani Campus, 94000 Pattani, Thailand
[3]Synchrotron Light Research Institute, Muang District, 30000 Nakhon Ratchasima, Thailand
[4]Rubber Engineering & Technology Program, International College, Prince of Songkla University, Hat Yai, 90110 Songkhla, Thailand

Received 30 May 2022; accepted in revised form 10 September 2022

Abstract. This study aimed to explore the best cross-link agent for preparing natural rubber (NR) composites containing sepiolite as filler. Three types of vulcanizing agents, namely, sulfur, peroxide, and phenolic resin, were employed, and their effects on the thermomechanical and mechanical properties and microstructures were investigated. Compared to other vulcanizing agents, the greatest thermomechanical and mechanical properties improvement was achieved by using phenolic resin as a crosslinker. The highest tensile stress and tensile strength improvement were also achieved from the phenolic resin system. Tensile strength was improved by approximately 78%, nearly twice as much as that in the sulfur system. Such drastic improvement was attributed to the combined effect of homogeneity dispersion and strong adhesion between rubber and filler, as revealed by Fourier-transform infrared spectroscopy, facilitating the strain-induced crystallization process in NR. The phenolic resin was the best vulcanizing agent for preparing NR/sepiolite composites.

Keywords: *polymer composites, rubber, vulcanizing agents, sepiolite filler*

1. Introduction

Natural rubber (NR) is not used as an engineering product unless it is cross-linked and reinforced with fillers. Aside from achieving appropriate performance characteristics for end-use applications, incorporating a filler is a simple, effective, and generally inexpensive method for enhancing the properties of rubber products [1–4]. Various types of filler have been applied in rubber composites, with carbon black and silica being the most widely used fillers in the rubber industries [1, 2].

Recently, the use of sepiolite as filler in rubber composites has been the subject of research due to the unique structure of sepiolite, allowing for the enhancement of mechanical, thermal, and barrier performance of composites [5–7]. Sepiolite, a naturally occurring material, is a hydrous magnesium silicate with the conceptual unit cell formula of $Si_{12}Mg_8O_{30}(OH,F)_4{\cdot}(H_2O)_4{\cdot}8H_2O$. It is a 2:1 phyllosilicate structural family having a fibrous morphology with a length of about 0.2–4 μm. The structure of the sepiolite has a tunnel-like micropore channel and has silanol groups (Si–OH) at the edges of the tunnel, allowing for effective adsorption and improved interaction with the rubber matrix [8, 9].

It has been reported that incorporating sepiolite by milling technique enhanced the properties of the composites, such as curing, mechanical, thermal,

*Corresponding author, e-mail: abdulhakim.m@psu.ac.th

swelling, flammability, and morphological properties [5]. Di Credico *et al*. [10] have prepared NR/sepiolite composites by using the latex-compounding technique and found that this approach provided more uniformity of sepiolite distribution in the rubber matrix. The dynamic mechanical properties of NR/sepiolites were greater than those of composites prepared using the conventional milling approach. However, the mechanical properties, *i.e.*, tensile and curing properties, were not reported. Recently, Hayeemasae *et al*. [7] have investigated the effect of sepiolite addition procedures (mill and latex mixing approaches) on the properties of the NR/sepiolite composites. They have discovered that the conventional milling method improved composite properties due to better rubber–filler interactions attributed to the nature of sepiolite, which does not swell in water like other types of clay.

To our best knowledge, the effect of vulcanizing agents on the properties of NR/sepiolite composites has not been reported. Since the sepiolite contained Si–OH groups on its surface, determining the best vulcanizing agents for this composite is of interest. In this study, the NR/sepiolite composites containing three different vulcanizing agents, namely, sulfur, peroxide, and phenolic resin, were prepared. Thermomechanical and tensile properties were investigated using temperature scanning stress relaxation (TSSR) and tensile test. The microstructure changes were investigated using small-angle and wide-angle X-ray diffraction (SAXS, WAXS). The dispersion of sepiolite filler was examined by using a scanning electron microscope (SEM), and Fourier-transform infrared spectroscopy (FTIR) was used to clarify the interaction between NR and filler. The possibility of properties enhancement for various composites was discussed.

2. Experimental setup

2.1. Materials

NR-graded STR 5L was supplied by Chalong Concentrated Natural Rubber Latex Industry Co., Ltd., Songkhla, Thailand. Zinc oxide (ZnO, 99%) was purchased from Global Chemical Co., Ltd., Samut Prakan, Thailand. Stearic acid was purchased from Imperial Chemical Co., Ltd., Bangkok, Thailand. Sepiolite clay, having the main compositions of [wt%]; SiO_2 (55%), Al_2O_3 (15%), Fe_2O_3 (3%) with traces of water, was produced by Guangzhou Billion Peak Chemical Technology Co., Ltd., Guangzhou, China. The sulfur (S, 99%) cross-link agent and its accelerator, dibenzothiazole disulfide (MBTS, 96%), were supplied by Siam Chemical Co., Ltd., Samut Prakarn, Thailand, and Shanghai Rokem Industrial Co., Ltd., Shanghai, China, respectively. Dicumyl peroxide (DCP, 40%) crosslinker and its coagent, triallyl isocyanurate, (TAIC, 98%), were purchased from Wuzhou International Co., Ltd., Shenzhen, China, and Sigma-Aldrich, Inc., Missouri, USA, respectively. Phenolic resin cross-link agent containing methylol content of 6.0–9.0% (HRJ-10518) and its catalyst, stannous chloride ($SnCl_2$, 98%), were supplied by Schenectady International Inc., New York, USA, and KemAus, New South Wales, Australia, respectively.

2.2. Rubber composite preparation

NR and NR/sepiolite composites with various vulcanizing agents, including sulfur (S), peroxide (P), and phenolic resin (Ph), were prepared using a laboratory-size internal mixer (Plastograph EC, Brabender GmbH & Co., Duisburg, Germany) with a mixing chamber of 55 cm^3. The chemical ingredients listed in Table 1 were added in the order shown in Figure 1. The NR with and without stearic acid and ZnO were initially mixed for 3 min in an internal mixer at a rotor speed of 60 rpm and 40 °C of mixer temperature. It should be noted here that stearic acid and ZnO were used as activators for the S cross-link system. After that, the sepiolite filler was added to the mixture and mixed for 5 min. Next, the curing promotor (MBTS, TAIC, or $SnCl_2$) was fed to the mixing chamber and allowed to mix for 1 min. Finally, a curing agent (S, DCP, or Ph) was added to the mixture and mixed for 1 min. After completion of the mixing with a total mixing time of 10 min, the

Table 1. Compound formulations for NR and its composite compounds.

Chemicals	Quantity [phr]		
	S-Sep 10	P-Sep 10	Ph-Sep 10
NR	100	100	100
Stearic acid	1		
ZnO	3		
Sepiolite clay	0 and 10	0 and 10	0 and 10
MBTS	1.5		
S	1.5		
TAIC		1.5	
DCP		1.5	
$SnCl_2$			1
Phenolic resin			10

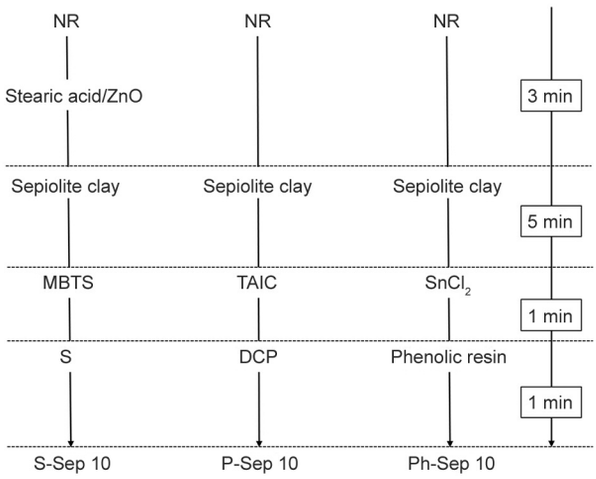

Figure 1. Sequence of chemical addition.

rubber compounds were then cross-linked through compression molding (SLLP-50, Siam Lab, Nonthaburi, Thailand) at 160 °C, following their respective curing times (t_{90}) to obtain 1 mm thick cross-linked sheets. The NR composite containing 10 phr sepiolite samples cross-linked with sulfur, peroxide, and phenolic resin systems were noted as S-Sep 10, P-Sep 10, and Ph-Sep 10, respectively, while their unfilled counterparts were indicated as S, P, and Ph, respectively.

2.3. Rubber composite characterization

2.3.1. Curing properties

The curing characteristics of rubber compounds were determined using a moving die rheometer (MDR 3000 Basic, Montech, Buchen, Germany) at 160 °C. The minimum torque (M_L), maximum torque (M_H), torque difference ($M_H - M_L$), scorch time (t_{S1}), and cure time (t_{90}) parameters were reported.

2.3.2. Fourier-transform infrared spectroscopy (FTIR)

Attenuated total reflectance–Fourier-transform infrared (ATR-FTIR) spectra of all samples were characterized using a Spotlight 200i spectrometer (Perkin Elmer, Inc., Massachusetts, USA). Each spectrum was recorded with resolutions of 4 cm^{-1} from 4000 to 400 cm^{-1}.

2.3.3. Thermomechanical properties and cross-link density

The thermomechanical properties and cross-link density of NR and its composites were measured using the temperature scanning stress relaxation (TSSR) meter, (Brabender, Duisburg, Germany). The dumbbell-shaped test specimens (ISO 527, type 5A) of NR composites and neat NR were placed in the heating chamber and stretched for 50% at 23 °C. After 2 hours, the specimens were subjected to a nonisothermal test at a heating rate of 2 °C/min until the specimens were ruptured.

The apparent cross-link density (ν) can be estimated from the maximum slope in the initial part of the stress temperature curve using the Equation (1) [11]:

$$\nu = \frac{\kappa}{R(\lambda - \lambda^{-2})} \tag{1}$$

where R is the universal gas constant, λ is the nominal strain ratio, and κ is the temperature coefficient of stress which can be defined as the derivative of mechanical stress (σ) as a function of temperature (T) as Equation (2) [11]:

$$\kappa = \left(\frac{\partial \sigma}{\partial T}\right)_{\lambda,p} \tag{2}$$

where, from the theory of rubber elasticity, the σ is directly proportional to the absolute T, and this relationship can be shown as Equation (3) [11]:

$$\sigma = \frac{\rho RT}{M_c}(\lambda - \lambda^{-2}) \tag{3}$$

were, ρ denotes the mass density, R is the universal gas constant, λ signifies the extension ratio ($\lambda = L/L_0$, where L and L_0 are the final and initial length of the sample, respectively), and M_c is the average molar weight of the elastically active network chains, which is inversely proportional to the ν of the networks according to the following correlations (Equation (4)):

$$M_c = \frac{\rho}{\nu} \tag{4}$$

By combining Equations (2) and (3), the value of ν at constant strain can be finally calculated from the slope of stress versus temperature as previously expressed in Equation (1).

2.3.4. Tensile properties

The tensile properties, including stress at 100 and 300% strains, tensile strength, and strain at break of the composites with and without sepiolite filler, were determined at 500 mm/min according to ISO 37 (Type 2) using universal testing equipment, LR5K Plus (Lloyd Instruments, West Sussex, UK). The dumbbell-shaped test specimens with a thickness of

2 mm and an overall length of test specimens of 75 mm were used in this study.

2.3.5. Microstructural properties

Microstructural changes, *i.e.*, distribution of sepiolite filler in the cross-linked samples and crystallization during stretching, were investigated using small-/wide-angle X-ray scattering, SAXS/WAXS measurement. Moreover, SAXS and WAXS measurements were performed at the BL1.3W:SAXS/WAXS, Siam Photon Laboratory, Synchrotron Light Research Institute, Nakhon Ratchasima, Thailand. The WAXD and SAXS data were taken during continuous stretching at a 500 mm/min crosshead speed. The SAXSIT data processing program was employed to normalize and rectify all WAXD and SAXS data.

The degree of crystallinity [%] corresponding to the (200) plane was estimated using the Equation (5) [12]:

$$\text{Crystallinity [\%]} = \frac{A_c}{A_c + A_a} \quad (5)$$

where A_c denotes the area below the 200 crystalline peaks and A_a denotes the amorphous halo area. The average crystallite sizes corresponding to (200) planes were estimated from the Scherrer equation [13] (Equation (6)):

$$\text{Crystalline size} = \frac{K\lambda}{\beta \cos\theta} \quad (6)$$

where K is equal to 0.89, λ is the wavelength, β is the half width at half height, and θ is the Bragg angle.

Structural changes, *e.g.*, dispersion of cross-link network structures in NR and distributions of the filler in the composites with different vulcanizing agents, were analyzed by using SAXS measurements. Two-dimensional (2D) SAXS images were background corrected and then integrated to obtain the scattering intensity (I) as a function of the scattering vector (q). The q is defined as Equation (7):

$$q = \frac{4\pi \sin\theta}{\lambda} \quad (7)$$

where λ is the wavelength and 2θ is the scattering angle.

2.3.6. Morphological properties

Scanning electron microscopy (SEM) (Quanta 400, Thermo Fisher Scientific, Brno-Cernovice, Czech Republic) was used to analyze the dispersion of sepiolite clay filler in the NR matrix containing various vulcanizing agents. The samples were fractured in liquid nitrogen before sputter coating with gold to minimize electrostatic charge buildup during testing.

3. Results and discussion

3.1. Curing properties

The curing characteristics of NR and its composite compounds with various cross-link agents are displayed in Table 2. It was seen that the M_L, the indirect indicator of a compound viscosity, M_H, the modulus of fully cross-linked composites, and $M_H - M_L$, the distinction between the shear moduli of cross-linked and uncrosslinked composites, increased with the incorporation of sepiolite clay filler. Because the sepiolite has a high aspect ratio and surface area [9], the high surface area of the filler provides a more favorable surface for the filler to interact with the polymer chains for interacting with the rubber molecules. Physical interactions between rubber chain segments adsorbing on filler surfaces served as additional cross-links in composites, restricting the rubbery matrix chain mobility. Consequently, the stiffness of the composites has been enhanced [14]. Aside from the difference between the shear moduli before and after cross-linked and composites, $M_H - M_L$ can be

Table 2. Minimum torque (M_L), maximum torque (M_H), torque difference ($M_H - M_L$), scorch time (t_{S1}), and cure time (t_{90}) of NR and its composites with different vulcanizing agents.

Sample	Curing parameters				
	M_L [dN·m]	M_H [dN·m]	$M_H - M_L$ [dN·m]	t_{S1} [min]	t_{90} [min]
S	3.90±0.01	17.12±0.03	13.22±0.02	1.59±0.00	6.04±0.01
S-Sep 10	4.10±0.01	18.36±0.06	14.26±0.06	2.97±0.11	9.44±0.07
P	3.09±0.02	21.65±0.03	18.56±0.01	0.60±0.03	11.82±0.01
P-Sep 10	3.61±0.01	23.61±0.02	20.00±0.02	0.71±0.03	14.47±0.03
Ph	3.73±0.01	20.82±0.02	17.09±0.01	0.93±0.50	16.03±0.03
Ph-Sep 10	3.80±0.05	22.51±0.02	18.71±0.02	0.88±0.03	15.91±0.08

determined the relative cross-link density of rubber. The relative cross-link density of rubber composites increased with the incorporation of sepiolite filler. In the composite, the increase of cross-link density has resulted from good rubber–filler interactions [15, 16]. t_{S1} and t_{90} indicate the commencement of vulcanization and the time required to achieve 90% of the M_H value, respectively [17]. Except for the phenolic resin system, t_{S1} and t_{90} of NR composites cross-linked with sulfur and peroxide systems were longer than those of the neat cross-linked NR counterparts. Such observation can be attributed to the small fraction of chemical cross-links being absorbed in the structural tunnels of sepiolite [6, 18]. Considering the composite cross-linked with the phenolic resin system, both t_{S1} and t_{90} were slightly reduced, implying that the curing reaction occurred faster when the sepiolite was added. This decrease was probably attributed to the competitive interaction between phenolic resin with rubber chains (cross-link reaction) and phenolic resin with sepiolite filler, as will be discussed later.

3.2. Fourier-transform infrared spectroscopy (FTIR)

Figure 2 depicts the FTIR spectra of pure sepiolite and NR/sepiolite composites with different vulcanizing agents in the wavenumber range of 400–4000 cm^{-1} (Figure 2a), 3000–4000 cm^{-1} (Figure 2b), and 400–1200 cm^{-1} (Figure 2c). For comparison, the spectra of their unfilled counterparts were also included. From Figure 2a, the characteristic peaks at approximately 428, 469, and 535 cm^{-1} in pure sepiolite were particularly assigned to Si–O–Si bending vibration, whereas the broadband centered at 1031 cm^{-1} corresponded to the stretching of Si–O [19]. The band at 3690 and 3627 cm^{-1} were ascribed to the

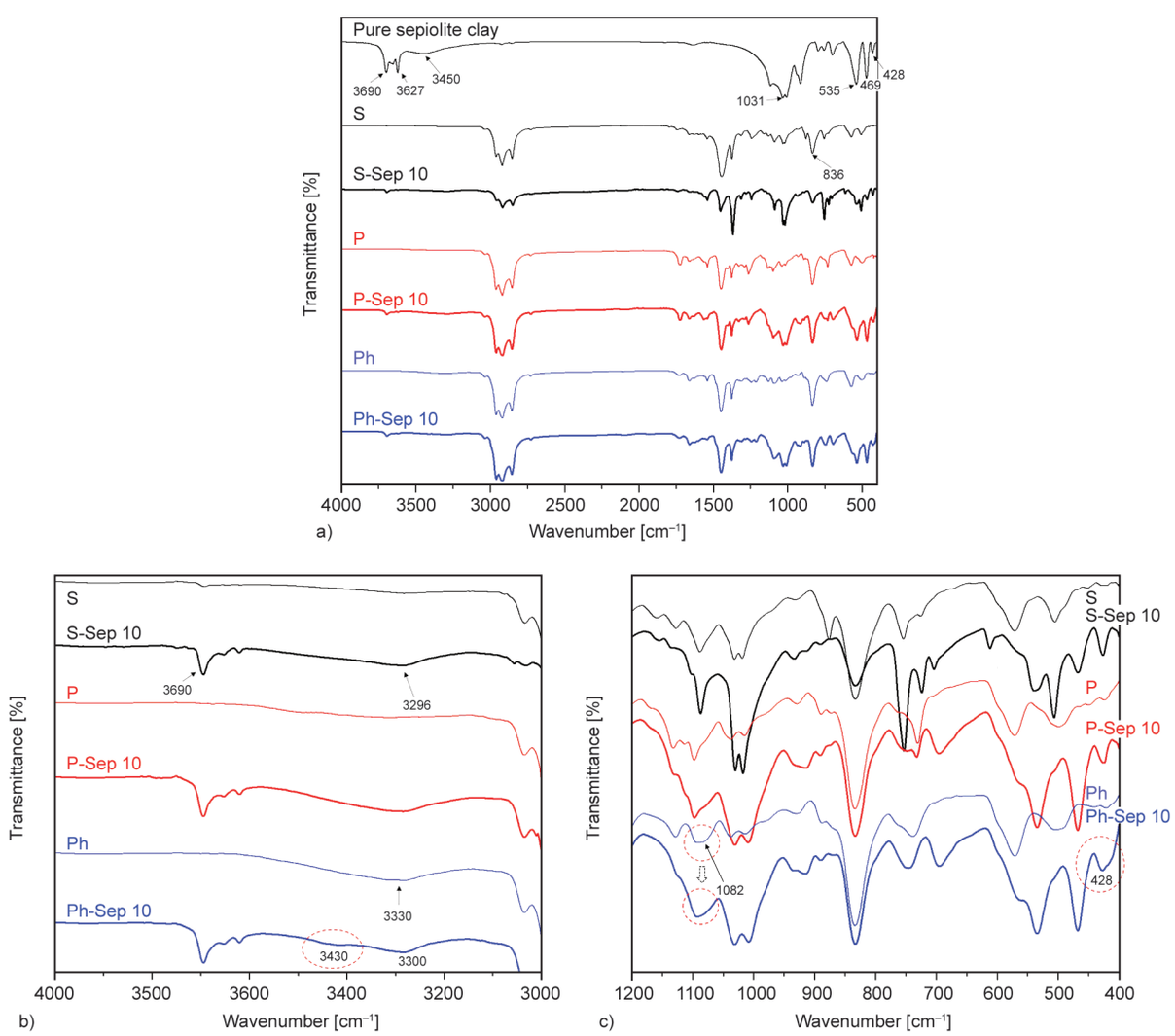

Figure 2. FTIR spectra of NR and its composites with different vulcanizing agents in the wavenumber range of a) 400–4000 cm^{-1}, b) 3000–4000 cm^{-1}, and c) 400–1200 cm^{-1}.

OH groups in the octahedral sheet and the OH stretching vibration in the external surface of sepiolite, and the broad peak centered at 3450 cm^{-1} in the range of 3600–3200 cm^{-1} was attributed to OH stretching of the zeolitic water in the sepiolite channels [19, 20]. For the NR cross-linked with sulfur (S), peroxide (P) and phenolic resin (Ph), the important characteristic peak of cross-linked NR was found at 837 cm^{-1}, which was associated with the out-of-plane bending vibration of C–H in the –CH=CH– group of cis-1,4-unit [6, 21]. With the exclusion of the Ph sample, all NR cross-linked with other systems did not exhibit a peak in the bands between 4000 and 3000 cm^{-1} (Figure 2b). The peak at 3330 cm^{-1} found in the Ph sample was attributed to –OH vibration of phenolic resin [22]. Up on the addition of sepiolite to the NR, the peak assigned to the OH stretching of sepiolite (3690 cm^{-1}) and –OH stretching from the zeolitic water (3296 cm^{-1}) were observed in all composites, indicating the presence of sepiolite dispersion in the rubber matrix. The phenolic resin cross-linked composites (Ph-Sep 10) caught the attention since they showed two peaks at 3430 and 3300 cm^{-1}, while these two peaks were not found in the composites cross-linked with peroxide (P-Sep 10) and sulfur (S-Sep 10) systems. When compared to those Ph, P, and S-Sep 10 samples, it was more likely that the –OH groups in Ph-Sep 10 had different chemical environments, indicating the probability of a hydrogen bonding (H-bond) between the –OH groups of the phenolic resin and the –OH groups of the sepiolite filler.

Considering the peak at 428 cm^{-1} in different composites (Figure 2c), a significant change was found in the spectrum of the Ph-Sep 10 compared to those of P-Sep 10 and S-Sep 10. The Ph-Sep 10 had a shoulder and broad peak at 428 cm^{-1}, whereas the others had simply a single sharp peak. Additionally, the broad peak at 1082 cm^{-1} due to C–O stretching in phenolic resin found in the Ph sample was also sharpened in Ph-Sep 10. These findings revealed that the O–Si–O and C–O present in the Ph-Sep 10 had different chemical environments when compared with those of P-Sep 10, S-Sep 10, Ph, and pure sepiolite. The OH group of phenolic resin ($–CH_2OH$) in the cross-linked precursor might chemically react with the silanol group (–SiOH) located at the edges surface of sepiolite. It is widely accepted that many silanol groups (–SiOH) are located along the margins of the sepiolite structure [8, 9], whereas the phenolic resin contains a hydroxyl (–OH) as a functional group. These two groups can interact with one other at molding temperatures (160 °C) via chemical bonding between silanol groups (–SiOH) located at the sepiolite edges and the OH group of phenolic resin, resulting in a Si–O–C bond, whereas hydrogen bonding is possible at low temperatures. According to the reports [22, 23], the peak for the Si–O–C bond appears at 1085 cm^{-1}, which may merge with the broad peak at 1082 cm^{-1} in this study. The presence of both the Si–O–C bond and the hydrogen bond was previously reported in composites composed of NR/clay nanocomposites [22], epoxidized natural rubber-(ENR-) silica [23], and ENR-sepiolite [24]. The presence of additional hydrogen bonding at low temperatures would result in the improvement of various properties. These hydrogen bonds would not affect the rheometer torque at vulcanization temperature because they exhibited temperature-dependent behavior, *i.e.*, they disintegrate at elevated temperatures [25]. As a result, the t_{90} of Ph and Ph-Sep 10 were almost comparable. Figure 3 depicts a possible interaction between the phenolic resin and sepiolite through the formation of hydrogen bonding and the Si–O–C bond. In addition to the cross-link reaction, these interactions would serve as an extra cross-linking point, resulting in faster scorch and cure times.

3.3. Thermomechanical properties and cross-link density

Figure 4 illustrates the normalized force curves of NR and its composites with different vulcanizing agents as a function of temperature obtained from temperature scanning stress relaxation (TSSR) measurement. At temperatures of 30–50 °C, the initial normalized force of all samples increased slightly due to the entropy effect [26, 27]. A slight reduction of force at 50–100 °C was probably due to the detachment of physical bonding among rubber molecules or between rubber and filler. At temperatures above 100 °C, the force abruptly decreases toward zero due to chain scission, and cleavage of network bridges between rubber molecules caused by thermo-oxidative reaction occurs [28]. Depending on the cross-linked systems, the force at any given temperature of cross-linked NR was shifted to a higher temperature. In the case of sulfur cross-linked NR, the decrement of force was found at a lower temperature than those of peroxide and phenolic systems due to lower bonding dissociation energy of the cross-linked

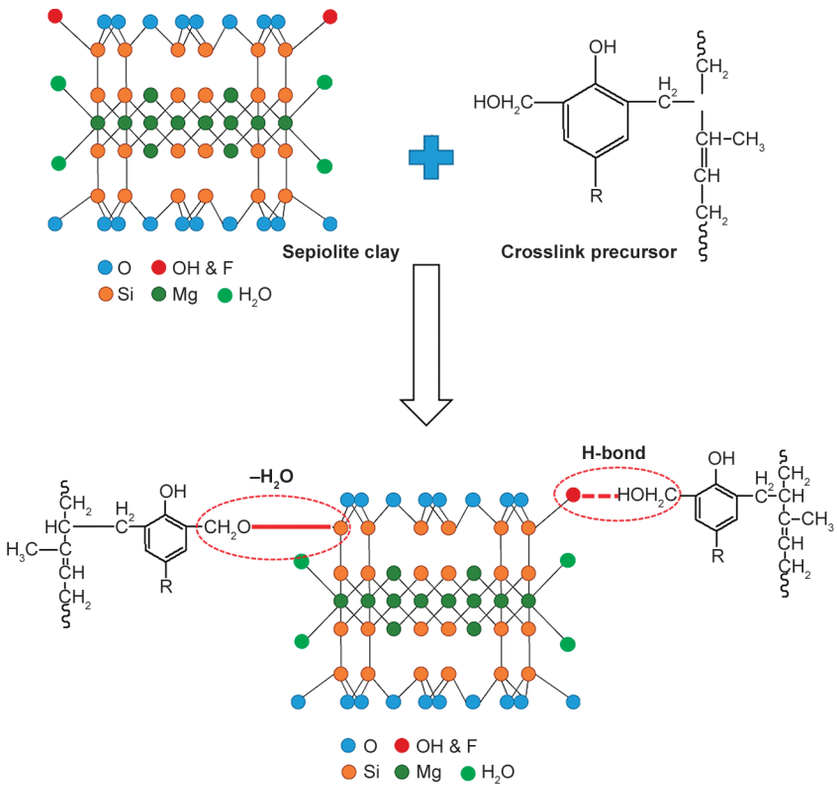

Figure 3. The probable mechanism of interactions between phenolic resin and sepiolite filler.

generated by the sulfur system, *i.e.*, monosulfidic (C–S–C; 285 kJ/mol), disulfidic (C–S–S–C; 268 kJ/mol), and polysulfidic (C–S–Sx–C; 252 kJ/mol) [29, 30]. In contrast, the C–C bonds generated from peroxide and phenolic systems provide a bear bonding energy of 344 kJ/mol, having higher dissociation energy than those of sulfidic cross-links [29, 31]. Therefore, the rubber cross-linked with the sulfur system had a more readily network bridge breakdown at elevated temperatures than peroxide and phenolic systems.

Moreover, the incorporation of sepiolite slightly shifted the force reduction toward higher temperatures compared to their unfilled counterparts at 120–170 °C. This was attributed to the sepiolite acting as a thermal insulator and as the mass transport barrier to the volatile products generated during decomposition [32]. The parameters obtained from TSSR measurement in terms of initial stress (σ_0) and the temperature at which the force ratio was reduced to 10, 50, and 90% (T_{10}, T_{50}, and T_{90}) concerning the initial force value [11], are shown in Table 3.

Table 3 shows that T_{10}, T_{50}, and T_{90} of the NR were enhanced by adding sepiolite due to the thermal insulator characteristic of the filler, as previously mentioned. Furthermore, the sepiolite filler may

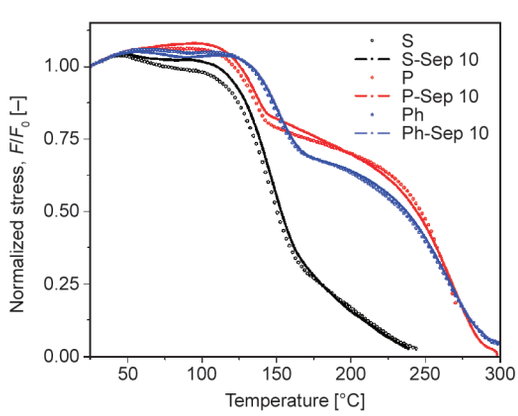

Figure 4. Normalized stress-temperature curves of NR and its composites with different vulcanizing agents.

Table 3. Initial stress (σ_0), the temperature at which the force ratio was reduced to 10, 50, and 90% with respect to the initial force value (T_{10}, T_{50}, and T_{90}), and cross-linked density (ν) of NR and its composites with different vulcanizing agents.

Sample	TSSR parameters				
	σ_0 [MPa]	T_{10} [°C]	T_{50} [°C]	T_{90} [°C]	ν [mol/m^3]
S	0.23	121.30	150.50	218.00	74.68
S-Sep 10	0.23	127.10	153.30	215.00	76.33
P	0.35	133.90	247.20	271.90	74.60
P-Sep 10	0.30	136.60	244.30	281.10	77.22
Ph	0.35	144.70	234.70	284.60	75.11
Ph-Sep 10	0.44	146.40	237.30	284.10	99.03

also adsorb some rubber chains, thereby retarding softening of the composites. It should be noted here that the T_{50} value in the P-Sep 10 was lower than in its unfilled sample, which was most likely due to poor dispersion and/or weak interaction between rubber and filler, as discussed later in the morphological properties section.

Considering σ_0 and cross-link density (ν) of various samples, a significant improvement of both σ_0 and ν was observed in the Ph-Sep 10. Compared to their counterparts, σ_0 and ν for the phenolic resin cross-linked NR/sepiolite composite were improved by about 25 and 30%, respectively, while other systems showed only a minor improvement. This vast improvement surely suggested the establishment of an additional bonding network between the phenolic and sepiolite fillers, retarding the motion of the rubber chains and strengthening the materials. It should be noted that the cross-link density of pure NR with various vulcanizing agents ranged from 74 to 75 mol/m^3, which was extremely low. As a result, the initial cross-link density obtained from these three systems can be assumed to be comparable and worthy of further comparison.

Figure 5 shows the time-dependent normalized stress (F/F_0) of NR and its composites with different vulcanizing agents during isothermal stress relaxation. This is an alternative approach to evaluating the rubber–filler interaction. Moreover, strong interaction between filler particles and rubber chains usually retarded the stress relaxation rate [7, 33]. Figure 5 shows that all composite samples showed a linearly decreasing trend of stress over time. A decrease in steep stress was observed in the S-Sep 10 and P-Sep 10 samples, implying that the molecular relaxation was very fast in these two samples. A lower stress relaxation rate was observed in the Ph-Sep 10, implying the stronger interaction between rubber and filler presented in this sample. This could be due to the formation of physical/chemical bonding between phenolic resin-NR and sepiolite filler, as shown in Figure 3.

3.4. Tensile properties

Figure 6 illustrates a typical stress-strain relationship for the pure NR and NR composites with various curing processes. Comparing to their unfilled counterparts, incorporating sepiolite into the NR enhanced the stress at given strains, and the strain where the steep increase of stress occurred was found at much lower strains. This finding revealed that introducing sepiolite increased the stress of NR, lowering the point of strain at the stress upturn.

The tensile properties in terms of 100% modulus (M100), 300% modulus (M300), tensile strength (TS), and elongation at break (EB) are listed in Table 4. The incorporation of sepiolite filler enhances the M100 and M300, which could be due to the hydrodynamic effect arising from the inclusion of rigid particles. The incorporation of sepiolite filler reduced the mobility of the rubber chains, resulting in more rigid, stiffer, and harder composites [34]. Additionally, an increase in the cross-linking density created by rubber–filler interactions was also another reason for the increase of the modulus [15], as previously suggested by $M_H - M_L$.

Likewise, the TS of the NR was found to increase with the addition of sepiolite. Masa *et al.* [6] have ascribed this improvement to a needle-like shape of sepiolite with a high aspect ratio, which offered considerable

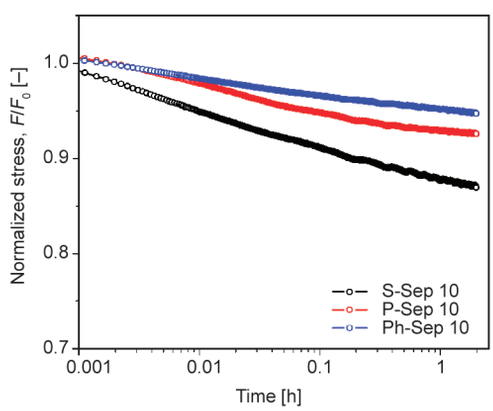

Figure 5. Normalized stress during isothermal stress relaxation of NR and its composites with different vulcanizing agents.

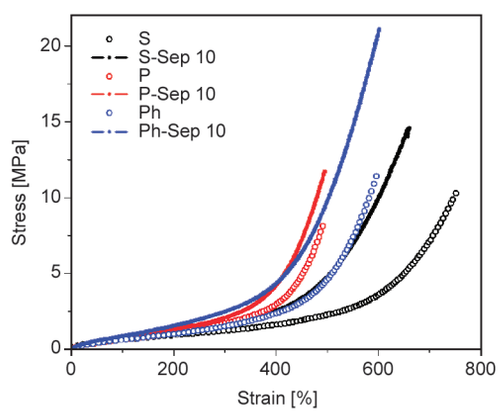

Figure 6. Representative stress-strain curves of NR and its composites with different vulcanizing agents.

Fsurface area to contact with the rubber, allowing for efficient stress transfer. Moreover, the rubber chains that possess linear chains can fit into the tight channels in the structure of sepiolite, causing a high interaction between sepiolite and NR [35].

It is worth highlighting that a massive increment in tensile modulus and TS was again noticed in the Ph-Sep 10 sample. The improvement of M100 and M300 in Ph-Sep 10 was about 43 and 69%, respectively, and the TS was about 78% compared to that of its unfilled sample, while the other vulcanizing agents (S-Sep 10 and P-Sep 10) showed only a slight improvement that was less than 35%. Such significant improvements noticed in the Ph-Sep 10 were attributed to a strong interaction between sepiolite and rubber due to the presence of phenolic resin, which resulted in improved stress transfer efficiency between the rubber matrix and the filler, resulting in greater modulus and TS. On the other hand, a slight improvement in the other vulcanizing agents could be attributed to the physical interaction between rubber and sepiolite filler. As a result of total cross-link density enhancement, the composites showed stiffer vulcanizates, limiting the deformation of the composites. Therefore, the EB of the composites was reduced.

Table 4. Tensile properties in terms of 100 and 300% modulus (M100 and M300), tensile strength (TS), and elongation at break (EB).

Sample	Tensile properties			
	M100 [MPa]	M300 [MPa]	TS [MPa]	EB [%]
S	0.66±0.03	1.29±0.10	10.42±0.01	766±19
S-Sep 10	0.70±0.07	1.67±0.01	14.04±2.08	688±80
P	0.63±0.01	1.72±0.04	8.21±0.81	497±12
P-Sep 10	0.78±0.04	2.08±0.09	11.02±0.68	490±11
Ph	0.61±0.02	1.49±0.14	11.90±0.14	606±14
Ph-Sep 10	0.87±0.01	2.52±0.08	21.19±0.72	588±13

3.5. Morphological properties

Scanning electron microscopic (SEM) analysis was performed to understand better the dispersion of sepiolite in an NR matrix comprising various vulcanizing agents. Figure 7 shows the micrographs of cryo-fractured surfaces of NR/sepiolite composites with various vulcanizing agents as observed through the SEM technique. The cross-link agents were discovered to have significantly impacted the dispersion of sepiolite filler (lighter dispersed phases) in the rubber matrix (darker background). The smallest size, from 0.25 to 6.00 µm, with the most homogeneous dispersion, was observed in the Ph-Sep 10 sample (Figure 7c), which was slightly better than that of the S-Sep 10 (Figure 7a).

The use of phenolic resin was presumably advantageous because the OH group in the phenolic resin may interact with the silanol groups (–SiOH) found on the sepiolite edges filler, as revealed by FTIR, causing homogeneity in sepiolite dispersion throughout the rubber matrix. This would almost certainly result in a significant improvement in the thermomechanical properties and mechanical properties of Ph-Sep 10. Although the sepiolite dispersion in S-Sep 10 and Ph-Sep 10 was slightly different, the increase in TS of Ph-Sep 10 was nearly double that of S-Sep 10 compared to their unfilled counterparts. This significant improvement could only be achieved through strong interaction between filler and rubber. On the other hand, several agglomerates with the size of about 0.50–20.00 µm with the poorest dispersion were seen in the P-Sep 10 sample (Figure 7b). Such large aggregation found in the P-Sep 10 would surely destroy adhesion between rubber and filler, which may cause a reduction of mechanical properties, such

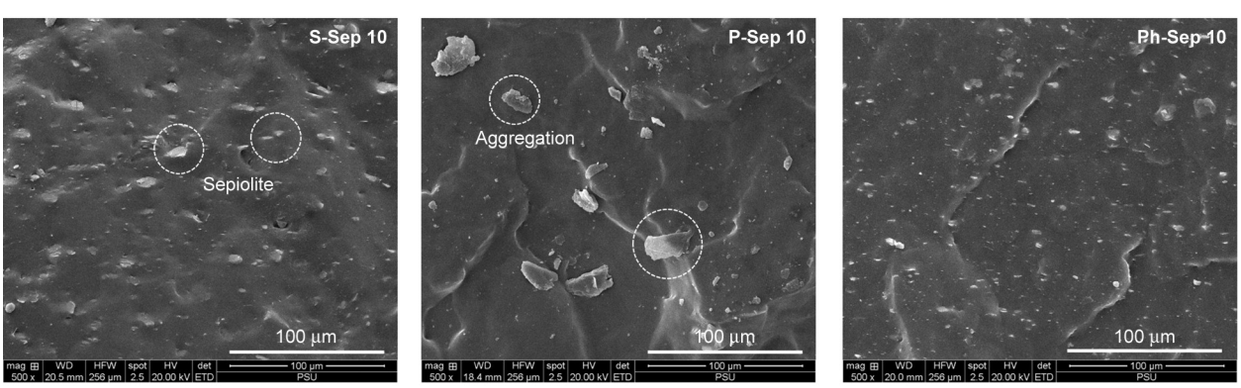

a) b) c)

Figure 7. SEM micrographs of a) S-Sep 10, b) P-Sep 10, and c) Ph-Sep 10.

as TS and EB of the composite samples. Poor dispersion of sepiolite in P-Sep 10 was probably attributed to part of the sepiolites being reaggregated during the vulcanization process. The related mechanism of this reaggregation is not clear at the moment. To clarify the aggregation of sepiolite during vulcanization, further investigation is required. However, similar behavior has been found in sulfur-crosslinked rubber/clay nanocomposites, and it was suggested that because of some organic cations were being ejected because of a probable reaction between the intercalant and vulcanizing agents [36, 37].

3.6. Microstructural properties

Figure 8 shows representative two-dimensional (2D) wide-angle X-ray scattering (WAXS) photographs of the composite sample (Ph-Sep 10) before (0% strain) and after deformation to 400% strain. Since no strain-induced crystallization occurs, no reflection spot was found for the sample before stretching (Figure 8a). When the strain-induced crystallization took place while stretching, various reflection spots were noticed due to the highly oriented crystal of NR induced by the stretching (Figure 8b). The most intense spots corresponded to different planes, *i.e.*, (200), (201), and (120). Among various intense reflection spots, the variation in crystallography corresponding to the (200) plane was investigated to evaluate the influence of sepiolite addition and types of cross-link agents on the microstructures of NR.

Figure 9 shows the degrees of crystallinity corresponding to the (200) planes of various cross-linked NR and composites. The crystallinity of all samples increased with increasing strain, proving that the crystallization of the NR was caused by deformation-induced crystallization. It is also seen that incorporating sepiolite filler increased the crystallinity of NR in all cases, depending on their dispersion. A significant enhancement of crystallinity was observed when

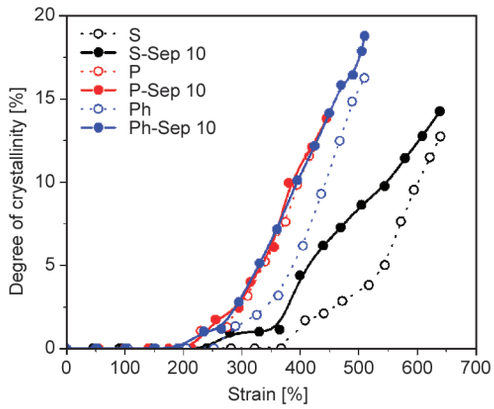

Figure 9. Degree of crystallinity at various strains in the NR and its composites with different vulcanizing agents.

the NR composites were cross-linked by sulfur and phenolic resin. As previously demonstrated in Figures 7a and 7c, good sepiolite filler dispersion in S-Sep 10 and Ph-Sep 10 significantly improved the crystallinity of NR due to high numbers of interfacial interactions (physical and/or chemical) between the NR chains and the filler. The presence of interfacial interactions would prevent the NR chain from moving, favoring alignment of the NR chains along the stretching direction, and resulting in more crystallinity [22, 38]. At the same strain, the crystallinity of Ph-Sep 10 was greater than that of S-Sep 10 due to the better interaction between rubber and filler phases. On the contrary, these interactions would be very limited in NR composites with poor filler dispersion (Figure 7b), preventing the rubber chains from aligning and crystallizing. Thus, the overall crystallinity of P-Sep 10 is not higher than that of unfilled rubbers. A reduction of crystallinity in NR composites with poor dispersion was also reported [38].

One may argue that less complexity in peroxide would provide a better change in crystallization compared to other systems. However, the addition of sepiolite makes the systems more complicated.

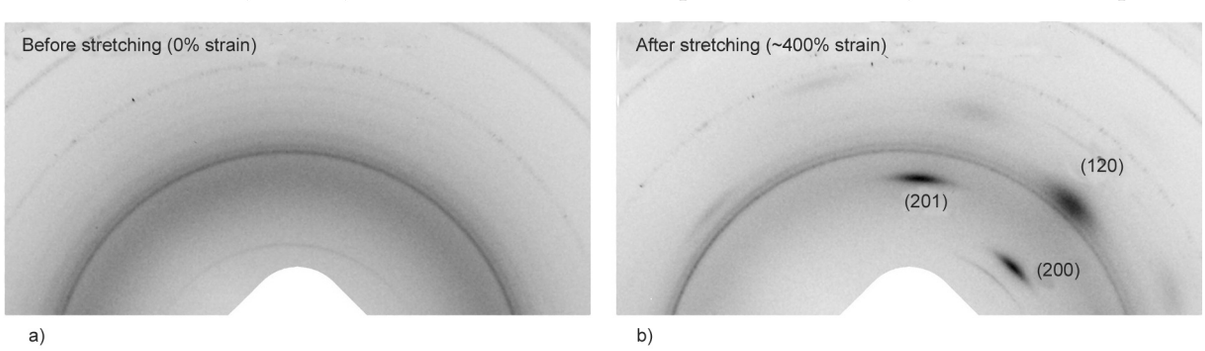

Figure 8. 2D WAXS images of the composite sample a) before and b) after stretching.

The introduction of filler in NR changes the stress field, increases the local strain of the chain, and leads to local heterogeneities [39]. Thus, the changes in various properties were more complicated even in a less complex peroxide system. In addition, the stain at which the crystallization took place was found at the lower strain in the composites, thus lowering the strain where the stress upturn occurred in the stress-strain curves when the unfilled samples were compared (Figure 6). This was probably attributed to the addition of the filler enhanced the network chain density, reducing then the distance between the cross-link points and shortening some rubber chains. These shorter chains are responsible for enhancing stain-induced crystallization at a small strain. Furthermore, the physical interaction between the filler and rubber chains is sufficient for improving the strain-induced crystallization of the NR [40]. The highest ability of strain-induced crystallization was observed in the Ph-Sep 10, where the highest TS was achieved. The strong rubber–filler interaction caused by the phenolic resin and sepiolite filler could clarify this phenomenon.

Considering the NR samples containing various vulcanizing agents, it was found that the type of cross-links formed in the rubber matrix has a significant effect on the crystallization process during stretching, although their cross-link densities (Table 3) were comparable. This suggested that the type of cross-link formation and distance between two cross-link points, as circled in Figure 10, could influence the strain-induced crystallization behavior. As previously suggested in the vulcanized NR with varied sulfur cross-link types (mono-, di- and polysulfidic) [41], short monosulfidic, or disulfidic linkages could better restrict the movement of the rubber chains compared to long polysulfidic linkages, accelerating, and enhancing the crystallization process. Therefore, the short and rigid structure of cross-links induced from the peroxide system (Figure 10b) may

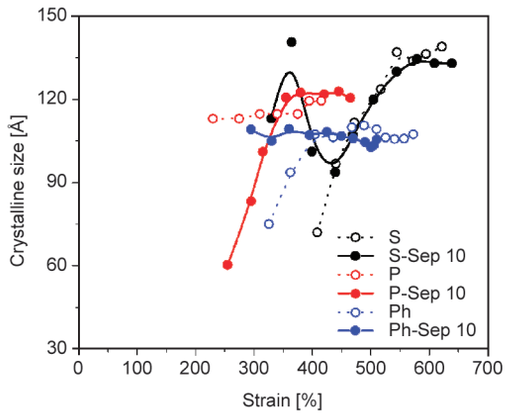

Figure 11. Variation of crystallite size at various strains in the NR and its composites with different vulcanizing agents.

better constrain the NR chain mobility, facilitating the orientation of the chains and thus enhancing the crystallization process during stretching. The highest crystallinity was found in the peroxide system, while the lowest crystallinity was observed in the sulfur system. It was reported that the NR cross-linked with peroxide exhibited a higher degree of crystallinity than the NR cross-linked with sulfur due to the peroxide system producing a more homogeneous network structure than the sulfur system [42].

Figure 11 displays the variation of crystalline size corresponding to the (200) plane at various strains in the NR and its composites with different vulcanizing agents. The crystallite size varied from approximately 60 to 130 Å, depending on the strains and vulcanizing agents. All the unfilled samples and composites showed a fluctuation in crystalline size with the variation in strains. It is believed that the strain-induced crystallization process involves two competing processes. Stretching, on the one hand, resulted in crystallite generation and crystallite growth, while on the other hand, declined crystallite formation and disappeared the generated crystallites. These events are thought to occur in a rubber matrix at random but more or less correlatively [42]. These two phenomena

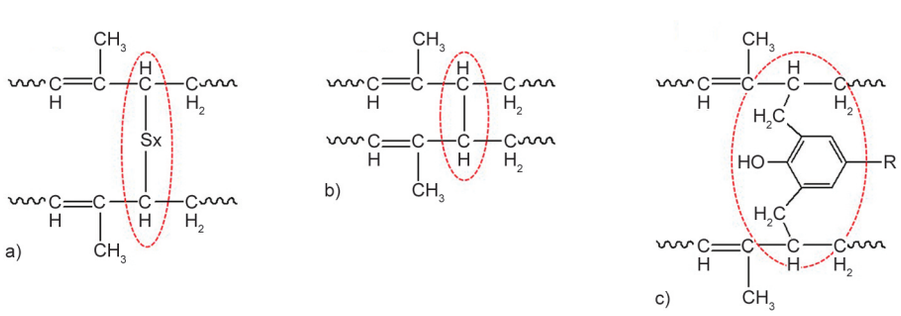

Figure 10. Cross-link formation from a) sulfur, b) peroxide and c) phenolic resin systems.

may result in the fluctuation in crystallite size during stretching. However, the changes in crystalline size were very small in the Ph-Sep 10. Such observation was probably attributed to the homogeneity of filler dispersion with strong rubber–filler interaction. To prove the homogeneity of filler dispersion in various samples, the small-angle X-ray scattering technique was applied.

Small-angle X-ray scattering (SAXS) measurements of all samples were performed to investigate the structures of the cross-link distribution and filler distributions [43]. A plot of the scattering intensity (I) against the scattering vector (q) of NR and its composites containing various vulcanizing agents is shown in Figure 12. Figure 12a shows that the scattering intensities of all unfilled NR with various vulcanizing agents showed a strong upturn in the low q region due to the heterogeneous network structures in the vulcanizates created by cross-linking network structures [44, 45]. Since the variation of scattering

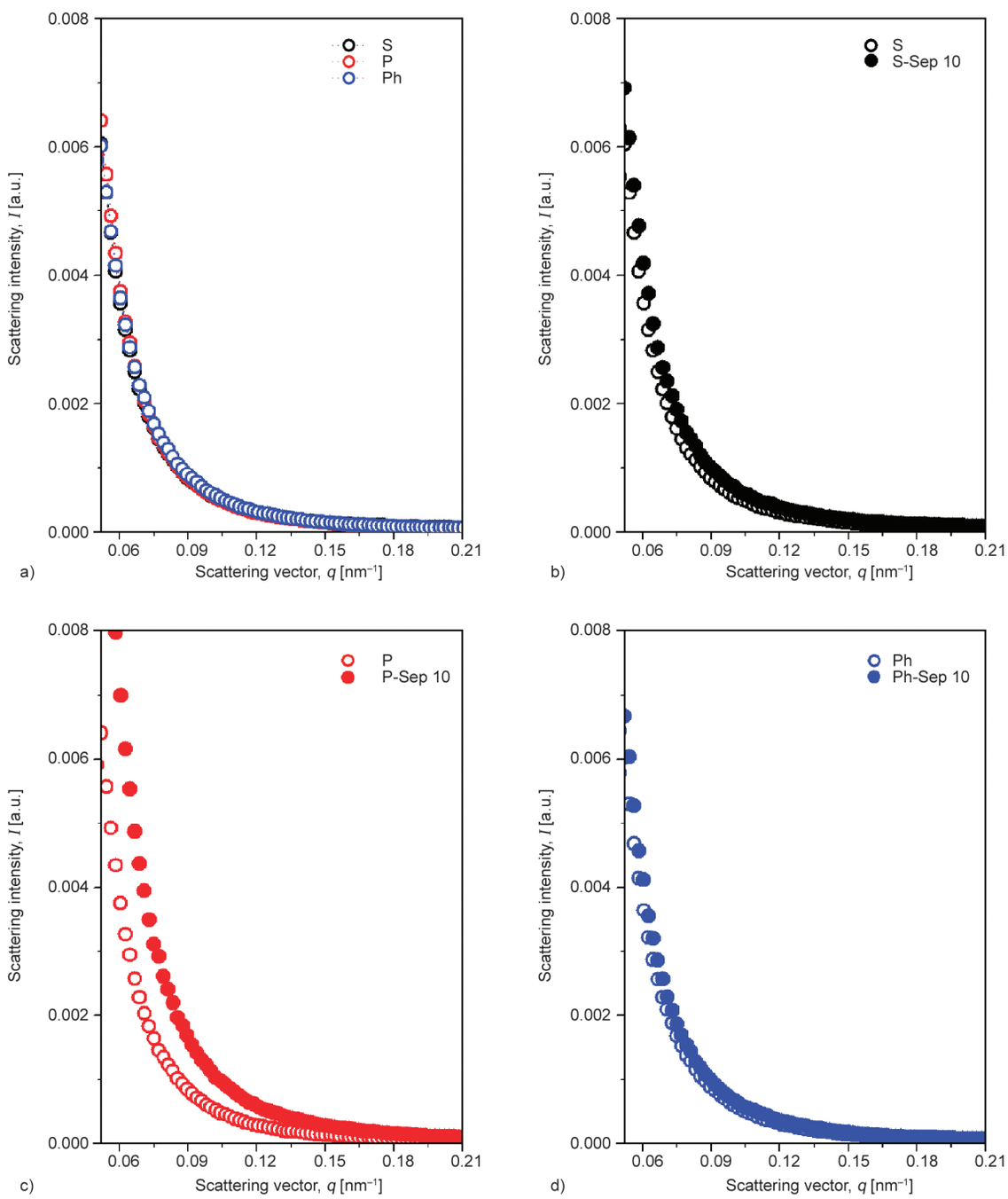

Figure 12. Correlation of the scattering intensity I with the scattering vector q for the a) unfilled NR samples and b) sulfur, c) peroxide, and d) phenolic resin cross-linked NR and their composites.

intensities of all unfilled samples were not significantly different, it can be assumed that the structure of cross-link networks with varied vulcanizing agents was almost similar. In the case of composites, there was a clear difference in scattering intensity between cross-linked NR and cross-linked composites. The SAXS intensity patterns for cross-linked composites displayed higher intensity than those of cross-linked counterparts (Figure 12b–12d). Therefore, the difference in the pattern of SAXS for cross-linked composites should be attributed to the presence of sepiolite filler. The presence of sepiolite altered the local electron density, which SAXS can detect. Notably, the scattering intensity of P-Sep 10 was substantially higher than that of the corresponding unfilled sample (Figure 12c), owing to poor sepiolite dispersion in the NR matrix, as evidenced by SEM (Figure 7), which causes high electron density fluctuation.

In contrast, the scattering intensity of the composites cross-linked with sulfur and phenolic resin (Figures 12b and 12d) remained nearly unaltered after the filler was added. Such phenomenon was attributed to the homogeneous dispersion with the smallest dimensions of sepiolite in the rubber matrix, as previously confirmed by SEM investigation. The SAXS results matched well with those obtained from the SEM observation.

4. Conclusions

In this study, composites of NR filled with sepiolite were prepared. The influence of several vulcanizing agents, including sulfur, peroxide, and phenolic resin, on the properties of the NR composites was investigated. Compared to other vulcanizing agents, the phenolic resin improved thermomechanical properties with the lowest stress relaxation rate. The highest tensile stress and TS were also achieved when the phenolic resin was used as a crosslinker. The enhancement was about 69% for tensile stress at 300% strains and about 78% for the TS. Such significant improvement was attributed to the homogeneity of small sepiolite dispersion with strong adhesion between rubber and filler through the assistance of phenolic resin, as suggested by FTIR. Such strong interaction facilitated the strain-induced crystallization process in the NR. The phenolic resin was the best vulcanizing agent for preparing NR composites containing sepiolite as filler.

Acknowledgements

This research was supported by Prince of Songkla University (Grant No. UIC6402030S).

References

[1] Bokobza L.: Natural rubber nanocomposites: A review. Nanomaterials, **9**, 12 (2019). https://doi.org/10.3390/nano9010012

[2] Roy K., Debnath S. C., Potiyaraj P.: A critical review on the utilization of various reinforcement modifiers in filled rubber composites. Journal of Elastomers and Plastics, **52**, 167–193 (2020). https://doi.org/10.1177/0095244319835869

[3] Chang B. P. P., Gupta A., Muthuraj R., Mekonnen T.: Bioresourced fillers for rubber composite sustainability: Current development and future opportunities. Green Chemistry, **23**, 5337–5378 (2021). https://doi.org/10.1039/D1GC01115D

[4] Maslowski M., Miedzianowska J., Strzelec K.: Natural rubber composites filled with crop residues as an alternative to vulcanizates with common fillers. Polymers, **11**, 972 (2019). https://doi.org/10.3390/polym11060972

[5] Zaini N. A. M., Ismail H., Rusli A.: Tensile, thermal, flammability and morphological properties of sepiolite filled ethylene propylene diene monomer (EDPM) rubber composites. Iranian Polymer Journal, **27**, 287–296 (2018). https://doi.org/10.1007/s13726-018-0609-6

[6] Masa A., Krem-ae A., Ismail H., Hayeemasae N.: Possible use of sepiolite as alternative filler for natural rubber. Materials Research, **23**, e20200100 (2020). https://doi.org/10.1590/1980-5373-MR-2020-0100

[7] Hayeemasae N., Adair A., Rasidi M. S. M., Jitsopin P., Masa A.: Influence of sepiolite addition methods and contents on physical properties of natural rubber composites. Science and Technology Indonesia, **7**, 140–148 (2022). https://doi.org/10.26554/sti.2022.7.2.140-148

[8] Kumar K. D., Tsou A. H., Bhowmick A. K.: Unique tackification behavior of needle-like sepiolite nanoclay in brominated isobutylene-*co*-p-methylstyrene (BIMS) rubber. Macromolecules, **43**, 4184–4193 (2010). https://doi.org/10.1021/ma100472r

[9] Mohanty T. R., Neeraj P., Ramakrishnan S., Amarnath S., Lorenzetti D., Mohamed P., Tyres A.: Sepiolite nanoclay: A reinforcing filler in the natural rubber/butadiene rubber (NR/BR) matrix for tire tread compound application. Rubber World, **263**, 32–44 (2021).

[10] Di Credico B., Tagliaro I., Cobani E., Conzatti L., D'Arienzo M., Giannini L., Mascotto S., Scotti R., Stagnaro P., Tadiello L.: A green approach for preparing high-loaded sepiolite/polymer biocomposites. Nanomaterials, **9**, 46 (2019). https://doi.org/10.3390/nano9010046

[11] Vennemann N., Bökamp K., Bröker D.: Crosslink density of peroxide cured TPV. Macromolecular Symposia, **245–246**, 641–650 (2006). https://doi.org/10.1002/masy.200651391

[12] Hernández M., López-Manchado M. A., Sanz A., Nogales A., Ezquerra T. A.: Effects of strain-induced crystallization on the segmental dynamics of vulcanized natural rubber. Macromolecules, **44**, 6574–6580 (2011). https://doi.org/10.1021/ma201021q

[13] Tosaka M., Murakami S., Poompradub S., Kohjiya S., Ikeda Y., Toki S., Sics I., Hsiao B. S.: Orientation and crystallization of natural rubber network as revealed by WAXD using synchrotron radiation. Macromolecules, **37**, 3299–3309 (2004). https://doi.org/10.1021/ma0355608

[14] Hayeemasae N., Adair A., Masa A.: Comparative study on viscosities, stress relaxation, curing and mechanical properties of sepiolite and silica filled natural rubber composites. Malaysian Journal of Analytical Sciences, **26**, 176–190 (2022).

[15] Bokobza L., Chauvin J-P.: Reinforcement of natural rubber: Use of *in situ* generated silicas and nanofibres of sepiolite. Polymer, **46**, 4144–4151 (2005). https://doi.org/10.1016/j.polymer.2005.02.048

[16] Kim D. Y., Park J. W., Lee D. Y., Seo K. H.: Correlation between the crosslink characteristics and mechanical properties of natural rubber compound via accelerators and reinforcement. Polymers, **12**, 2020 (2020). https://doi.org/10.3390/polym12092020

[17] Kopal I., Labaj I., Vršková J., Harničárová M., Valíček J., Ondrušová D., Krmela J., Palková Z.: A generalized regression neural network model for predicting the curing characteristics of carbon black-filled rubber blends. Polymers, **14**, 653 (2022). https://doi.org/10.3390/polym14040653

[18] Zadaka-Amir D., Bleiman N., Mishael Y. G.: Sepiolite as an effective natural porous adsorbent for surface oil-spill. Microporous and Mesoporous Materials, **169**, 153–159 (2013). https://doi.org/10.1016/j.micromeso.2012.11.002

[19] Frost R. L., Locos O. B., Ruan H., Kloprogge J. T.: Near-infrared and mid-infrared spectroscopic study of sepiolites and palygorskites. Vibrational Spectroscopy, **27**, 1–13 (2001). https://doi.org/10.1016/S0924-2031(01)00110-2

[20] Alkan M., Tekin G., Namli H.: FTIR and zeta potential measurements of sepiolite treated with some organosilanes. Microporous and Mesoporous Materials, **84**, 75–83 (2005). https://doi.org/10.1016/j.micromeso.2005.05.016

[21] Chen D., Shao H., Yao W., Huang B.: Fourier transform infrared spectral analysis of polyisoprene of a different microstructure. International Journal of Polymer Science, **2013**, 937284 (2013). https://doi.org/10.1155/2013/937284

[22] Masa A., Saito R., Saito H., Sakai T., Kaesaman A., Lopattananon N.: Phenolic resin-crosslinked natural rubber/clay nanocomposites: Influence of clay loading and interfacial adhesion on strain-induced crystallization behavior. Journal of Applied Polymer Science, **133**, 43214 (2016). https://doi.org/10.1002/app.43214

[23] Manna A. K., De P. P., Tripathy D. K., De S. K., Peiffer D. G.: Bonding between precipitated silica and epoxidized natural rubber in the presence of silane coupling agent. Journal of Applied Polymer Science, **74**, 389–398 (1999). https://doi.org/10.1002/(SICI)1097-4628(19991010)74:2<389::AID-APP21>3.0.CO;2-L

[24] Hayeemasae N., Zakaria N. H., Ismai H.: Epoxidized natural rubber/modified sepiolite composites. KGK Kautschuk Gummi Kunststoffe, **70**, 18–25 (2017).

[25] Wittenberg E., Meyer A., Eggers S., Abetz V.: Hydrogen bonding and thermoplastic elastomers – A nice couple with temperature-adjustable mechanical properties. Soft Matter, **14**, 2701–2711 (2018). https://doi.org/10.1039/C8SM00296G

[26] Vennemann N., Wu M.: Thermoelastic properties and relaxation behavior of S-SBR/silica vulcanizates. Rubber World, **246**, 18–23 (2012).

[27] Matchawet S., Kaesaman A., Vennemann N., Kumerlöwe C., Nakason C.: Effects of imidazolium ionic liquid on cure characteristics, electrical conductivity and other related properties of epoxidized natural rubber vulcanizates. European Polymer Journal, **87**, 344–359 (2017). https://doi.org/10.1016/j.eurpolymj.2016.12.037

[28] Srinivasan N., Bokamp K., Vennemann N.: New test method for the characterisation of filled elastomers. KGK Kautschuk Gummi Kunststoffe, **58**, 650–655 (2005).

[29] Bhowmick A. K., Mangaraj D.: Vulcanization and curing techniques. in 'Rubber products manufacturing technology' (eds.: Bhowmick A. K., Hall M. M., Benarey H. A.) Marcel Dekker, New York, 315–396 (1994).

[30] Gopi Sathi S., Harea E., Machů A., Stoček R.: Facilitating high-temperature curing of natural rubber with a conventional accelerated-sulfur system using a synergistic combination of bismaleimides. Express Polymer Letters, **15**, 16–27 (2021). https://doi.org/10.3144/expresspolymlett.2021.3

[31] Kruželák J., Sýkora R., Hudec I.: Sulphur and peroxide vulcanisation of rubber compounds – Overview. Chemical Papers, **70**, 1533–1555 (2016). https://doi.org/10.1515/chempap-2016-0093

[32] Chen H., Zheng M., Sun H., Jia Q.: Characterization and properties of sepiolite/polyurethane nanocomposites. Materials Science and Engineering: A, **445**, 725–730 (2007). https://doi.org/10.1016/j.msea.2006.10.008

[33] Maria H. J., Lyczko N., Nzihou A., Joseph K., Mathew C., Thomas S.: Stress relaxation behavior of organically modified montmorillonite filled natural rubber/nitrile rubber nanocomposites. Applied Clay Science, **87**, 120–128 (2014). https://doi.org/10.1016/j.clay.2013.10.019

[34] Pasbakhsh P., Ismail H., Fauzi M. A., Bakar A. A.: Influence of maleic anhydride grafted ethylene propylene diene monomer (MAH-*g*-EPDM) on the properties of EPDM nanocomposites reinforced by halloysite nanotubes. Polymer Testing, **28**, 548–559 (2009). https://doi.org/10.1016/j.polymertesting.2009.04.004

[35] Bhattacharya M., Bhowmick A. K.: Polymer–filler interaction in nanocomposites: New interface area function to investigate swelling behavior and Young's modulus. Polymer, **49**, 4808–4818 (2008). https://doi.org/10.1016/j.polymer.2008.09.002

[36] Wu Y-P., Ma Y., Wang Y-Q., Zhang L-Q.: Effects of characteristics of rubber, mixing and vulcanization on the structure and properties of rubber/clay nanocomposites by melt blending. Macromolecular Materials and Engineering, **289**, 890–894 (2004). https://doi.org/10.1002/mame.200400085

[37] Varghese S., Karger-Kocsis J., Gatos K. G.: Melt compounded epoxidized natural rubber/layered silicate nanocomposites: Structure-properties relationships. Polymer, **44**, 3977–3983 (2003). https://doi.org/10.1016/S0032-3861(03)00358-6

[38] Carretero-Gonzalez J., Retsos H., Verdejo R., Toki S., Hsiao B. S., Giannelis E. P., López-Manchado M. A.: Effect of nanoclay on natural rubber microstructure. Macromolecules, **41**, 6763–6772 (2008). https://doi.org/10.1021/ma800893x

[39] Chenal J-M., Gauthier C., Chazeau L., Guy L., Bomal Y.: Parameters governing strain induced crystallization in filled natural rubber. Polymer, **48**, 6893–6901 (2007). https://doi.org/10.1016/j.polymer.2007.09.023

[40] Masa A., Iimori S., Saito R., Saito H., Sakai T., Kaesaman A., Lopattananon N.: Strain□induced crystallization behavior of phenolic resin crosslinked natural rubber/clay nanocomposites. Journal of Applied Polymer Science, **132**, 42580 (2015). https://doi.org/10.1002/app.42580

[41] Sainumsai W., Suchiva K., Toki S.: Influence of sulphur crosslink type on the strain-induced crystallization of natural rubber vulcanizates during uniaxial stretching by *in situ* WAXD using a synchrotron radiation. Materials today: Proceedings, **17**, 1539–1548 (2019). https://doi.org/10.1016/j.matpr.2019.06.179

[42] Ikeda Y., Yasuda Y., Hijikata K., Tosaka M., Kohjiya S.: Comparative study on strain-induced crystallization behavior of peroxide cross-linked and sulfur cross-linked natural rubber. Macromolecules, **41**, 5876–5884 (2008). https://doi.org/10.1021/ma800144u

[43] Takenaka M.: Analysis of structures of rubber-filler systems with combined scattering methods. Polymer Journal, **45**, 10–19 (2013). https://doi.org/10.1038/pj.2012.187

[44] Osaka N., Kato M., Saito H.: Mechanical properties and network structure of phenol resin crosslinked hydrogenated acrylonitrile-butadiene rubber. Journal of Applied Polymer Science, **129**, 3396–3403 (2013). https://doi.org/10.1002/app.39010

[45] Masa A., Soontaranon S., Hayeemasae N.: Influence of sulfur/accelerator ratio on tensile properties and structural inhomogeneity of natural rubber. Polymer (Korea), **44**, 519–526 (2020). https://doi.org/10.7317/pk.2020.44.4.519